doi:10.1038/nature11417

Supplementary Table 1. Phenotypic characterization of ultradian rhythms in wild type (wt) heat stroke survivors after heat preconditioning

	Pharyngeal pumping*	Defecation†	Egg laying‡
Untreated animals (wt)	257±15	47±4.7	5.8±0.4
Heat stroke survivors (wt) after heat preconditioning	251±19	40.4±3.1	4.4±0.6

* Pumps per minute

† Duration of defecation cycle in seconds

‡ Number of eggs laid per worm, per hour

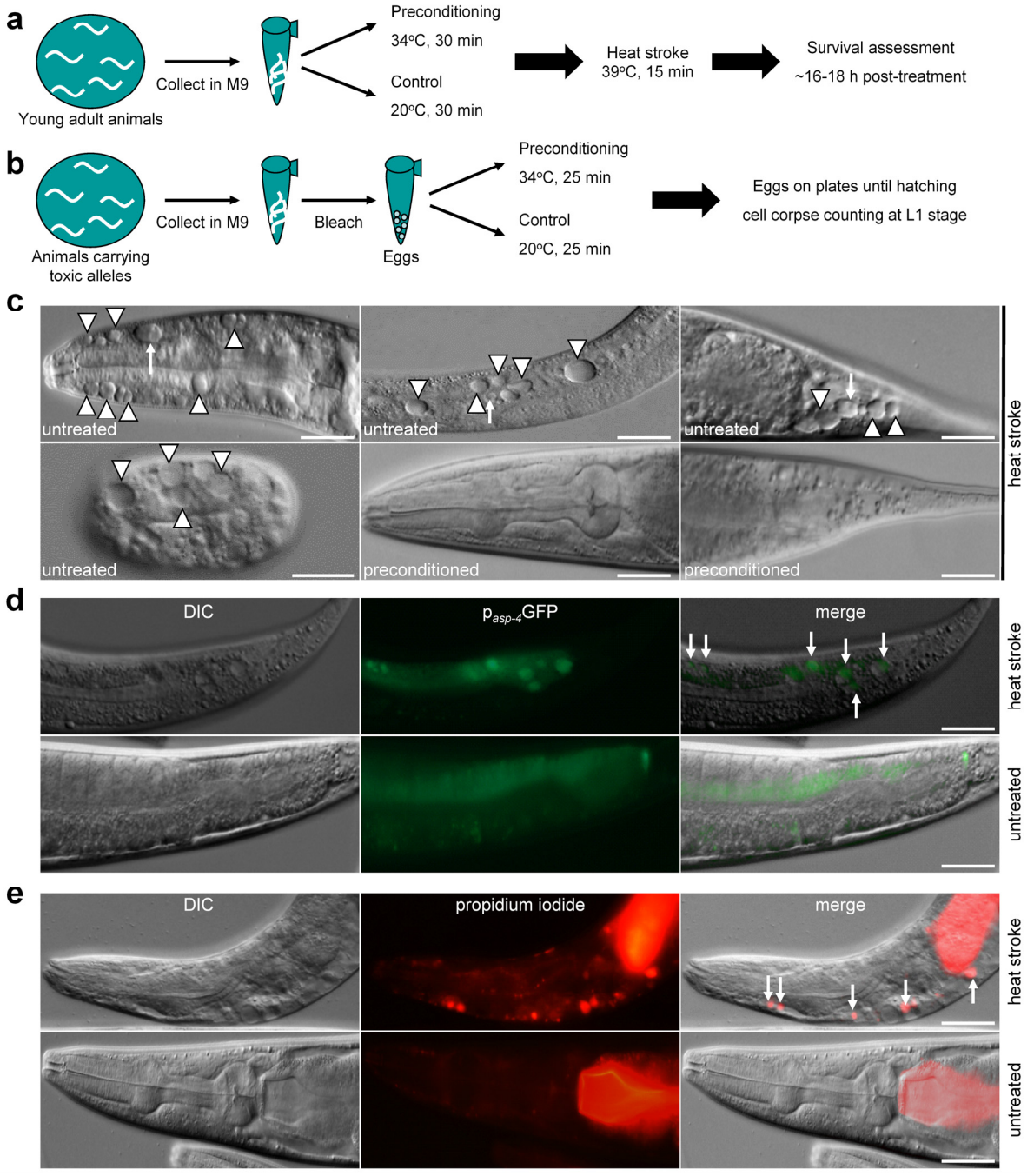

Figure S1 | Heat stroke conditions trigger necrotic cell death in *C. elegans*. a, Experimental procedure for administering heat stroke and heat preconditioning. **b,** Experimental procedure for administering heat preconditioning to animals carrying toxic alleles. **c,** DIC microscopy images of wild type animals after exposure to heat stroke. Dramatically swollen cells are observed throughout the bodies of the animals (top panels, arrowheads) and in embryos (bottom left panel, arrowheads). Distorted nuclei restricted in the periphery of vacuolated cells are indicated by arrows. Preconditioning protects animals from heat stroke-induced damage (bottom middle and right panels). Bar denotes 50 µm, white bar (egg) denotes 20 µm. **d,**

Transgenic animals carrying the reporter p_{asp-4}GFP after exposure to heat stroke (top panels). Arrows denote expression of the reporter inside vacuolated cells. Bar denotes 50 µm. **e,** Wild type animals stained with propidium iodide after exposure to heat stroke. Necrotic cells stained with propidium iodide due to loss of membrane integrity are indicated by arrows. Bar denotes 50 µm.

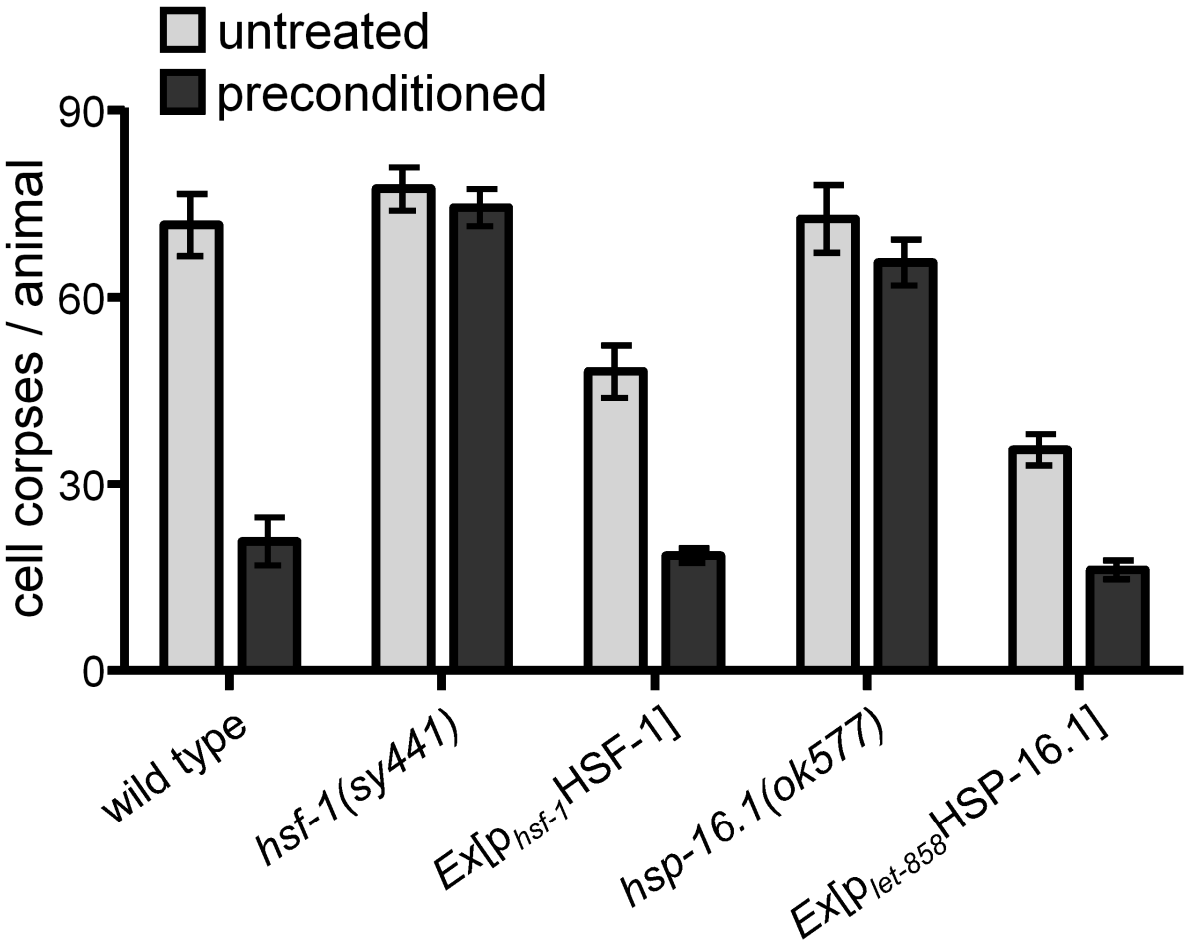

Figure S2 | Preconditioning protects against heat stroke-induced necrosis via HSF-1 and HSP-16. Number of cell corpses per animal, in wild type animals, *hsf-1(sy441)* mutants lacking HSF-1, transgenic animals overexpressing *hsf-1* (*Ex*[p_{hsf-1}HSF-1]), *hsp-16.1(ok577)* mutants lacking HSP-16.1, and transgenic animals overexpressing *hsp-16.1* (*Ex*[$p_{let-858}$HSP-16.1]) under heat stroke conditions, either without (untreated) or after heat preconditioning (N=100 animals per assay; P<0.001 for wt untreated vs. preconditioned, P>0.05 for *hsf-1(sy441)* or *hsp-16.1(ok577)* untreated vs. preconditioned, P<0.001 for wt untreated vs. *Ex*[p_{hsf-1}HSF-1] or *Ex*[$p_{let-858}$HSP-16.1] untreated; two-way ANOVA). Error bars denote standard error of the mean (S.E.M.) values.

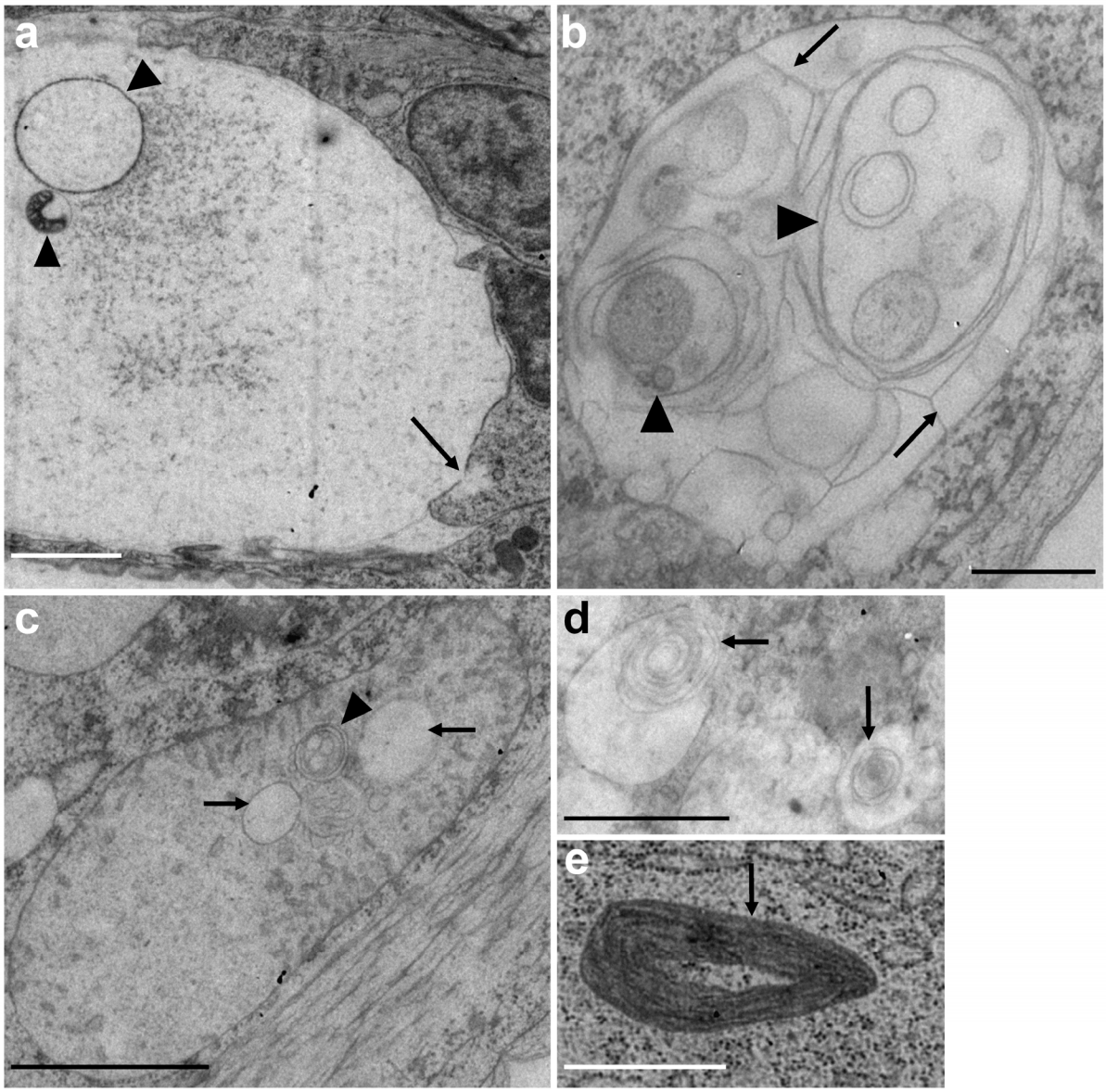

Figure S3 | Ultrastructural features of *C. elegans* cells after heat stroke. The morphology of various cell types in wild type animals subjected to heat stroke is shown in 50 nm HPF EM cross sections. **a,** Electron micrograph of a vacuolated neuron. Remnants of damaged organelles are observed (arrowheads). Note the break in the plasma membrane and the spill of the cell content (arrow). Bar denotes 2 µm. **b,** Electron micrograph of a cell in advanced degeneration. Huge vacuoles are invading the cell (arrowheads). Note the complex membrane derived network (arrows). Bar denotes 1 µm. **c,** Electron micrograph of a damaged mitochondrion. Membrane whorls (arrowhead) and vacuoles (arrows) are observed in the matrix. Bar denotes 1 µm. **d, e,** Membrane whorls (arrows) in intestinal (d), bar denotes 1 µm, and muscle cells (e), bar denotes 500 nm.

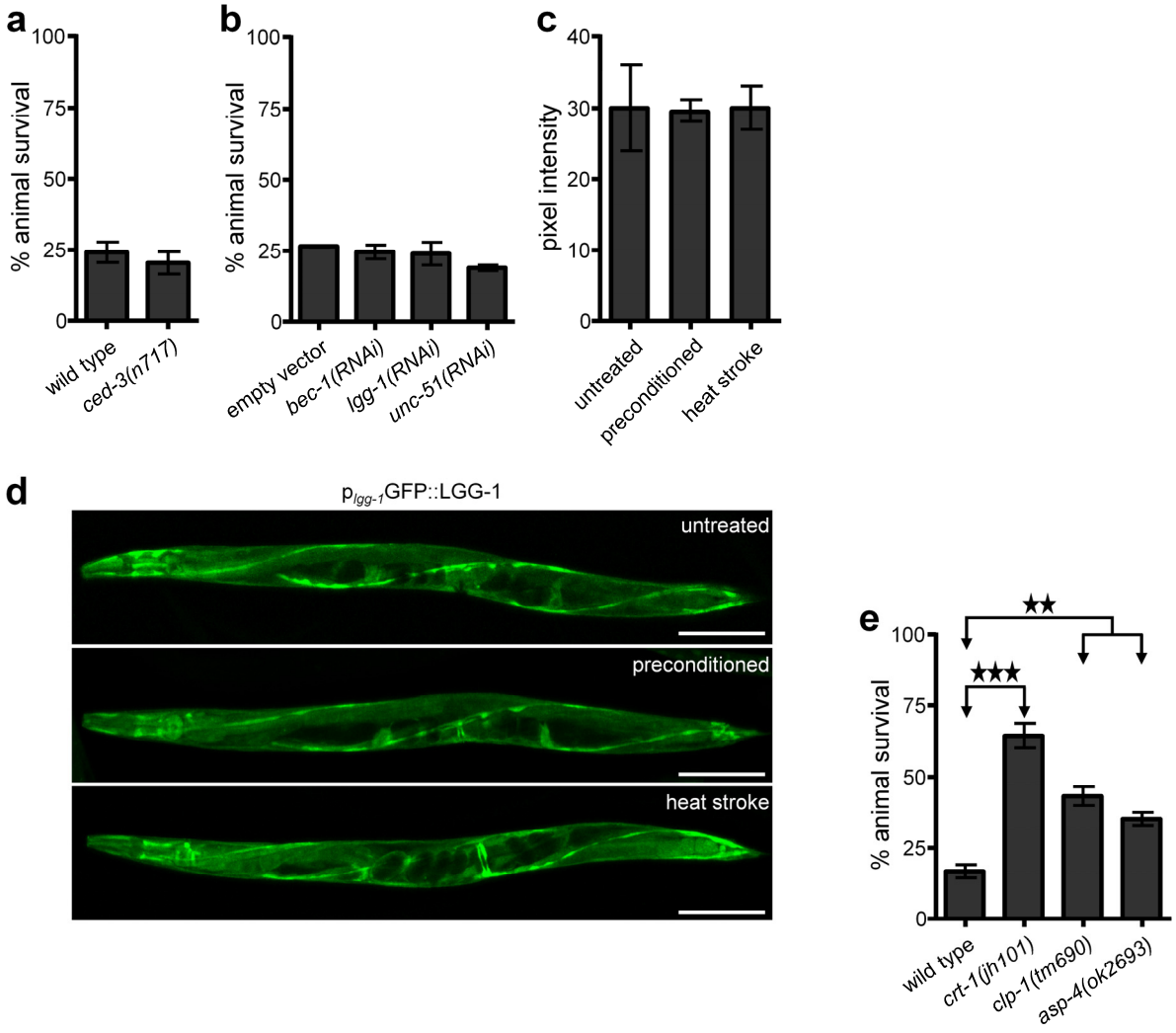

Figure S4 | Involvement for key mediators of apoptosis, autophagy and necrosis in heat stroke induced cell death. a, Survival of wild type animals and *ced-3(n717)* mutants deficient for the CED-3 caspase under heat stroke conditions (*N*=250 animals per assay; *P*>0.05 for wt vs. *ced-3(n717*; unpaired *t*-test). **b,** Survival of wild type animals and animals deficient for the Atg6/Vps30/Beclin1 homologue BEC-1 (*bec-1(RNAi)*), the autophagosome-associated ATG8/LC3/LGG-1 homologue LGG-1 (*lgg-1(RNAi)*), or the ATG1 homologue UNC-51 (*unc-51(RNAi)*) under heat stroke conditions (*N*=250 animals per assay; *P*>0.05 for wt vs. *bec-1(RNAi)* or *lgg-1(RNAi)* or *unc-51(RNAi)*; unpaired *t*-test). **c,** Fluorescence intensity of wild type animals expressing $p_{lgg\text{-}1}$GFP::LGG-1 transgene under control conditions (untreated), after heat preconditioning and after heat stroke (*N*=50 animals per assay; *P*>0.05 for wt untreated vs. preconditioned or heat stroked; unpaired *t*-test). **d,** Confocal images of transgenic animals expressing a full-length $p_{lgg\text{-}1}$GFP::LGG-1 reporter fusion under normal conditions (untreated; top panel), after preconditioning (middle

panel) and after heat stroke (bottom panel). Bar denotes 100 µm. **e,** Survival of wild type animals, *crt-1(jh101)* mutants deficient for the calreticulin CRT-1, *clp-1(tm690)* mutants deficient for the calpain protease CLP-1, and *asp-4(ok2693)* mutants deficient for the cathepsin protease ASP-4 under heat stroke conditions (*N*=350 animals per assay; *P*<0.001 for wt vs. *crt-1(jh101)*, *P*<0.01 for wt vs. *clp-1(tm690)* or *asp-4(ok2693)*; unpaired *t*-test). Error bars denote standard error of the mean S.E.M.

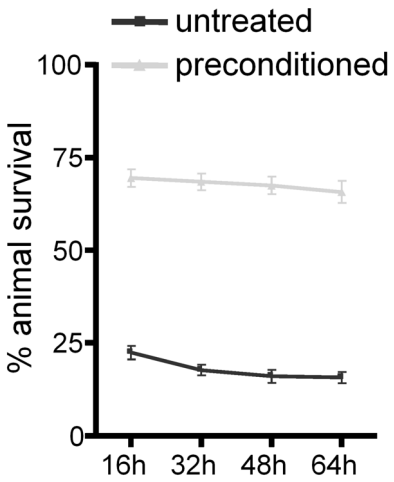

Figure S5 | Long term endurance of heat stroke survivors. Time-course analysis of survival of wild type animals under heat stroke conditions either without (untreated) or after heat preconditioning (*N*=300 animals per assay; *P*<0.001 for wt untreated vs. preconditioned; unpaired *t*-test). Error bars denote standard error of the mean (S.E.M.) values.

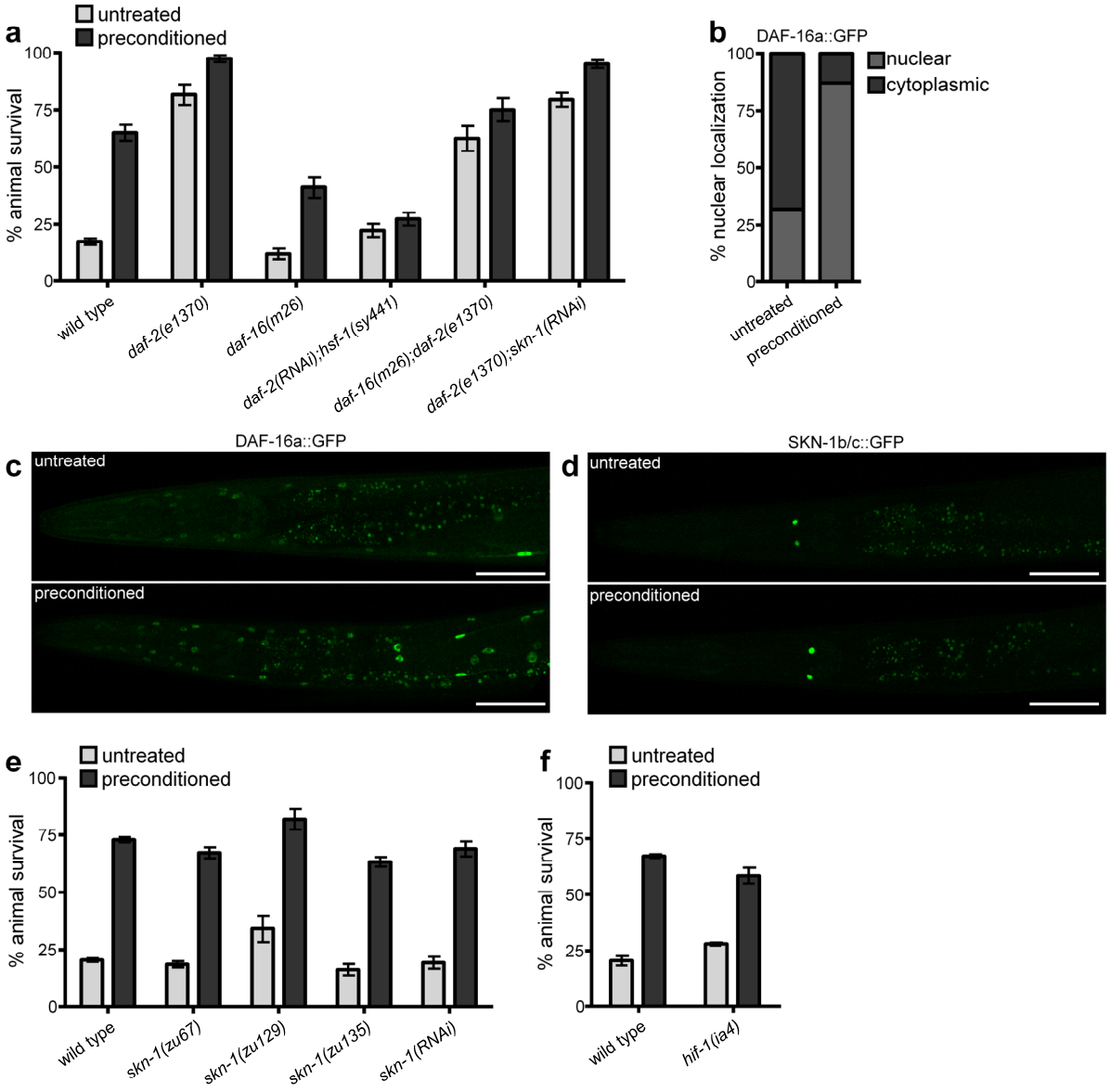

Figure S6 | Contribution of main stress related pathways in the survival after heat stroke. a, Survival of wild type animals, *daf-2(e1370)* mutants deficient for the DAF-2 insulin/insulin-like growth factor (IGF) receptor, *daf-16(m26)* mutants deficient for DAF-16, *daf-2(RNAi);hsf-1(sy441)* mutants deficient for DAF-2 and HSF-1, *daf-16(m26);daf-2(e1370)* mutants deficient for DAF-2 and DAF-16, and *daf-2(e1370);skn-1(RNAi)* mutants deficient for DAF-2 and SKN-1, under heat stroke conditions either without (untreated) or after heat preconditioning (*N*=350 animals per assay; *P*<0.001 for wt preconditioned vs. *daf-16(m26)* preconditioned, *P*<0.001 for *daf-2(e1370)* untreated vs. *daf-2(RNAi);hsf-1(sy441)* untreated, *P*<0.001 for wt untreated vs. *daf-16(m26);daf-2(e1370)* untreated, *P*>0.05 for *daf-2(e1370)* untreated vs. *daf-2(e1370);skn-1(RNAi)* untreated; two-way ANOVA). **b,** Nuclear accumulation of DAF-16 in animals expressing the p_{daf-16}DAF-16a::GFP transgene reporter fusion either without (untreated) or after heat preconditioning. **c,**

Confocal images of transgenic *daf-16(mu86)* mutants deficient for DAF-16, expressing the p_{daf-16}DAF-16a::GFP transgene reporter fusion under normal conditions (untreated, top panel) and after heat preconditioning (bottom panel). Bar denotes 50 μm. **d,** Confocal images of wild type transgenic animals expressing the p_{skn-1}SKN-1b/c::GFP transgene reporter fusion under normal conditions (untreated, top panel) and after heat preconditioning (bottom panel). Bar denotes 50 μm. **e,** Survival of wild type animals and *skn-1(zu67)*, *skn-1(zu129), skn-1(zu135)*, and *skn-1(RNAi)* animals deficient for SKN-1 under heat stroke conditions either without (untreated) or after heat preconditioning (*N*=250 animals per assay; *P*>0.05 for wt preconditioned vs. *skn-1(zu67)*, *skn-1(zu129), skn-1(zu135)*, and *skn-1(RNAi)* preconditioned; two-way ANOVA). **f,** Survival of wild type animals, and *hif-1(ia4)* mutants deficient for HIF-1 under heat stroke conditions either without (untreated) or after heat preconditioning (*N*=250 animals per assay; *P*>0.05 for wt preconditioned vs. *hif-1(ia4)* preconditioned; two-way ANOVA). Error bars denote S.E.M. values.

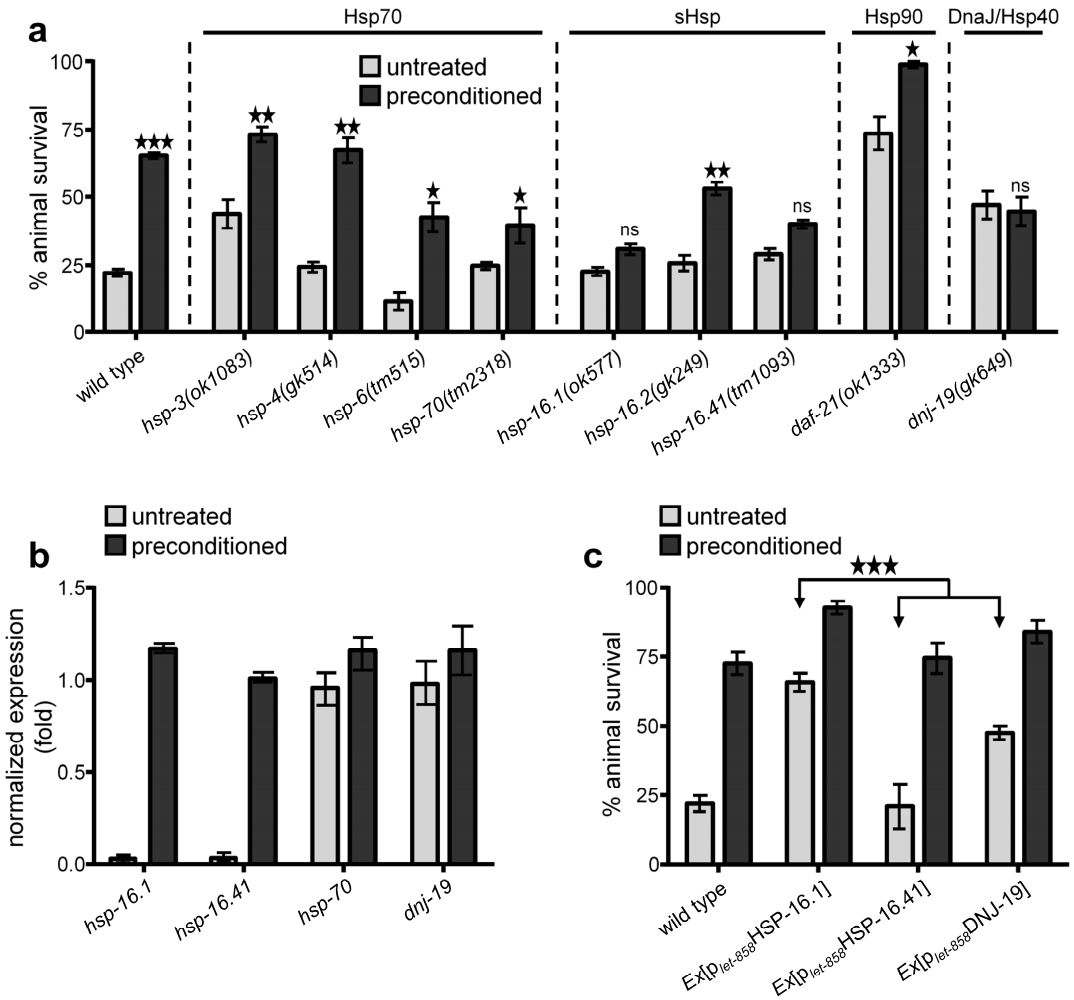

Figure S7 | Involvement of representative heat shock proteins in the protective preconditioning response. a, Exposure of mutants representing the four major classes of heat shock proteins to heat stroke either without (untreated) or after preconditioning: small heat shock proteins (HSPs) (*hsp-16.1(ok577)*, *hsp-16.2(gk249)*, *hsp-16.41(tm1093)*), Hsp70s (*hsp-3(ok1083)*, *hsp-4(gk514)*, *hsp-6(tm515)*, *hsp-70(tm2318)*), Hsp90 (*daf-21(ok1333)*) and DnaJ/Hsp40 (*dnj-19(gk649)*) (*N*=450 animals per strain; *P*<0.001 for wt untreated vs. preconditioned, *P*<0.01 for *hsp-3(ok1083)*, *hsp-4(gk514)* and *hsp-16.2(gk249)*, untreated vs. preconditioned, *P*<0.05 for *hsp-6(tm515)*, *hsp-70(tm2318)* and *daf-21(ok1333)* untreated vs. preconditioned, *P*>0.05 for *hsp-16.1(ok577)*, *hsp-16.41(tm1093)* and *dnj-19(gk649)* untreated vs. preconditioned; unpaired *t*-test; ns: not significant difference). **b,** Real time PCR analysis of *hsp-16.1*, *hsp-16.41*, *hsp-70*, and *dnj-19* mRNA levels in wild type animals, under normal conditions (untreated) or after heat preconditioning. **c,** Survival of wild type animals, transgenic animals overexpressing *hsp-16.1* (*Ex*[$p_{let-858}$HSP-16.1]), transgenic animals overexpressing *hsp-16.41* (*Ex*[$p_{let-858}$HSP-16.41]), and transgenic animals overexpressing *dnj-19* (*Ex*[$p_{let-858}$DNJ-19]) under heat stroke conditions either without (untreated) or after heat preconditioning (*N*=350 animals per assay; *P*<0.001 for *Ex*[$p_{let-858}$HSP-16.1] untreated vs. *Ex*[$p_{let-858}$HSP-16.41] or *Ex*[$p_{let-858}$DNJ-19] untreated; two-way ANOVA). Error bars denote S.E.M. values.

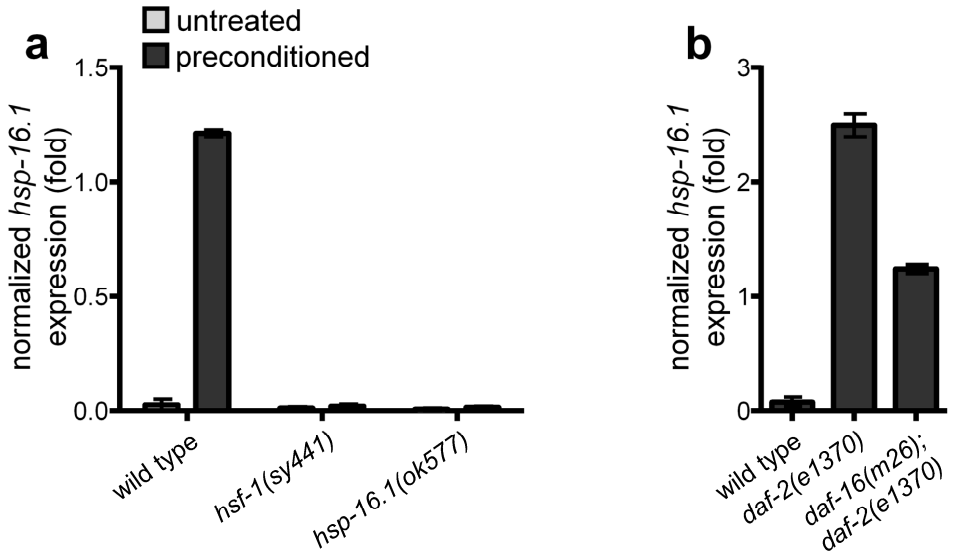

Figure S8 | *hsp-16.1* expression induction upon preconditioning is dependent on HSF-1. a, Real time PCR analysis of *hsp-16.1* mRNA levels in wild type animals, *hsf-1(sy441)* mutants lacking HSF-1, and *hsp-16.1(ok577)* mutants lacking HSP-16.1, under normal conditions (untreated) or after heat preconditioning (P<0.001 for wt preconditioned vs. *hsf-1(sy441)* or *hsp-16.1(ok577)* preconditioned; two-way ANOVA). **b,** Real time PCR analysis of *hsp-16.1* mRNA levels in wild type animals, *daf-2(e1370)* mutants deficient for DAF-2, and *daf-16(m26);daf-2(e1370)* mutants deficient for DAF-16 and DAF-2, under normal conditions. Error bars denote S.E.M. values.

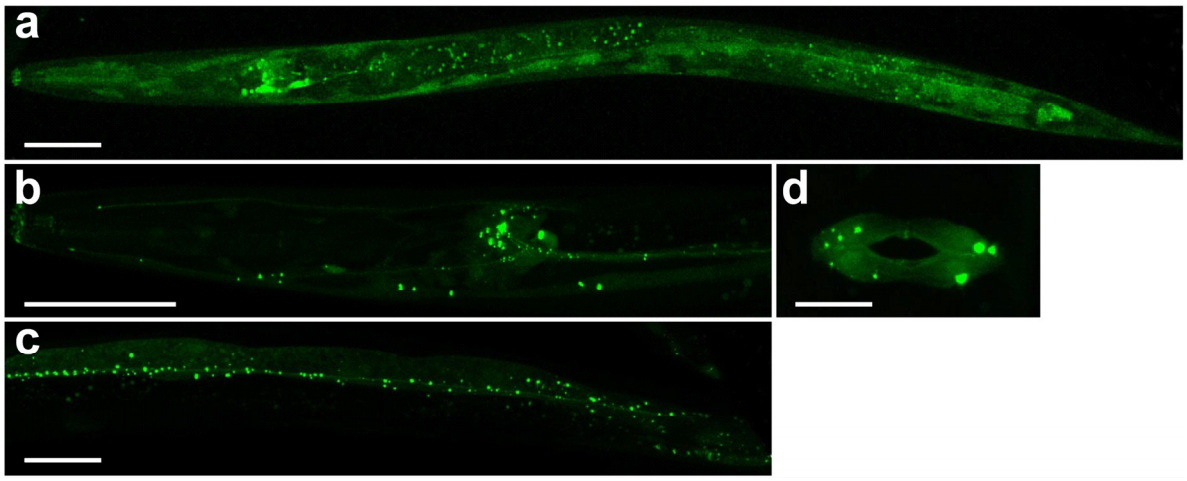

Figure S9 | HSP-16.1 subcellular localization. Images of transgenic animals expressing a full-length $p_{let-858}$HSP-16.1::GFP reporter fusion. *hsp-16.1* expression shows a punctuated, Golgi-like pattern in all tissues. **a,** General view of a transgenic animal at L4 stage. **b-d,** Focus on adult transgenic animals: head region (**b**), intestine (**c**) and vulva (**d**). Bar denotes 50 µm in all panels except **d**. In panel d, bar denotes 15 µm. Images were acquired using a 40x objective lens. Left is anterior and right is posterior.

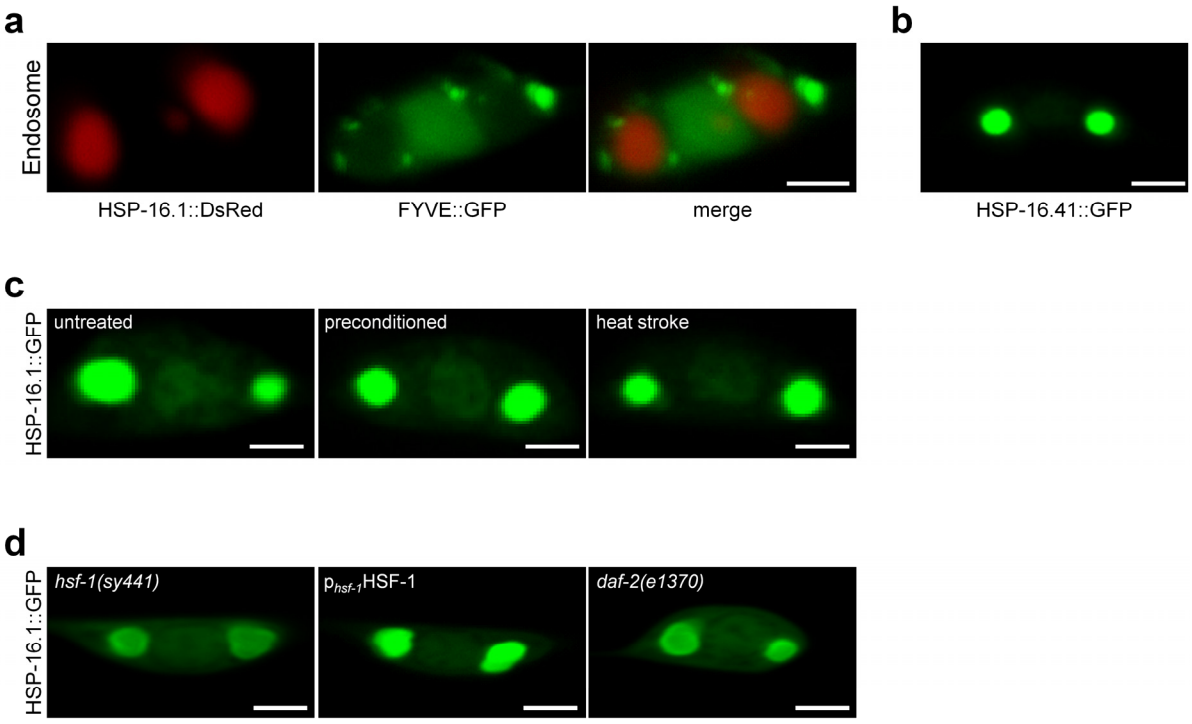

Figure S10 | HSP-16.1 does not localize in early endosomes and its localization is not influenced by preconditioning or heat stroke. a, Confocal images of touch receptor neuron cell bodies of wild type animals expressing fluorescently tagged (DsRed) HSP-16.1 along with a marker of early endosomes (GFP tagged). FYVE is a domain of EEA-1 (Early Endosome Antigen 1). **b,** Confocal image of a wild type touch receptor neuron cell body expressing fluorescently tagged (GFP) HSP-16.41. **c,** Confocal images of touch receptor neuron cell bodies of wild type animals expressing fluorescently tagged (GFP) HSP-16.1 under normal conditions (untreated), upon heat preconditioning or heat stroke. **d,** Confocal images of touch receptor neuron cell bodies of *hsf-1(sy441)* mutants lacking HSF-1, transgenic animals overexpressing *hsf-1* (*Ex*[p_{hsf-1}HSF-1]), and *daf-2(e1370)* mutants deficient for DAF-2, expressing fluorescently tagged (GFP) HSP-16.1. Images were acquired using a 63x objective lens. Size bars denote 4 µm.

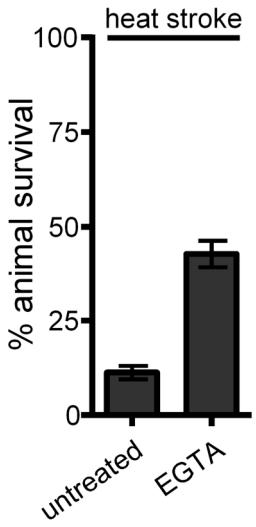

Figure S11 | The Ca^{2+} chelator EGTA protects from heat stroke-induced death. Survival of wild type animals (untreated) and animals treated with EGTA under heat stroke conditions (*N*=300 animals per assay; *P*<0.01 for wt untreated vs. EGTA treated; unpaired *t*-test). Error bars denote S.E.M. values.

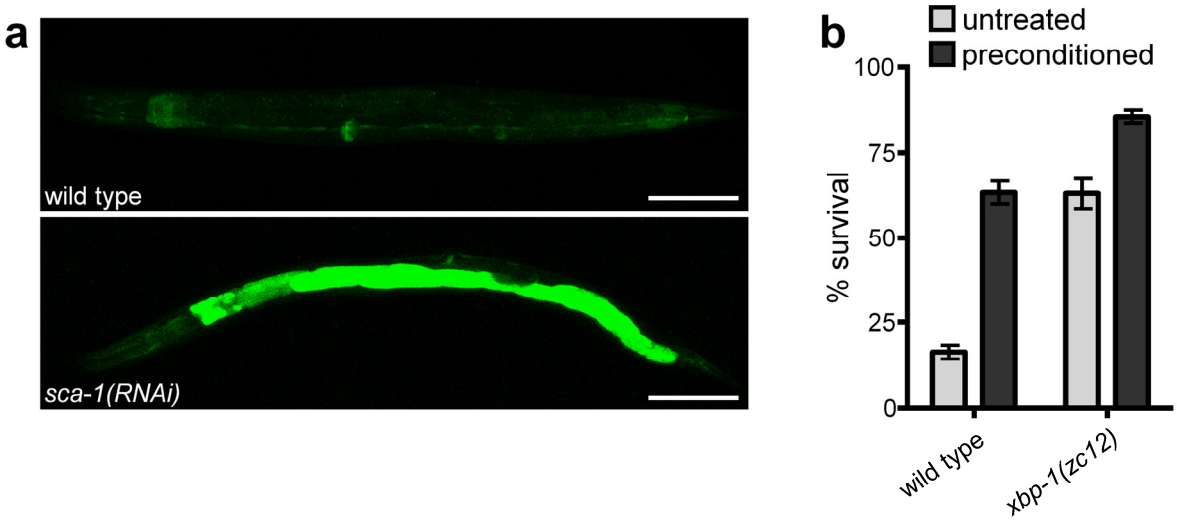

Figure S12 | Downregulation of SERCA activates the unfolded protein response (UPR). a, Confocal images of wild type transgenic worms expressing the reporter p_{hsp-4}GFP under normal conditions (top panel) and after downregulation of *sca-1* by RNAi (bottom panel). Bar denotes 100 µm. **b,** Survival of wild type animals, and *xbp-1(zc12)* mutants deficient for XBP-1 under heat stroke conditions, either without (untreated) or after heat preconditioning (*N*=350 animals per assay; *P*<0.001 for wt untreated vs. *xbp-1(zc12)* untreated; two-way ANOVA). Error bars denote S.E.M. values.

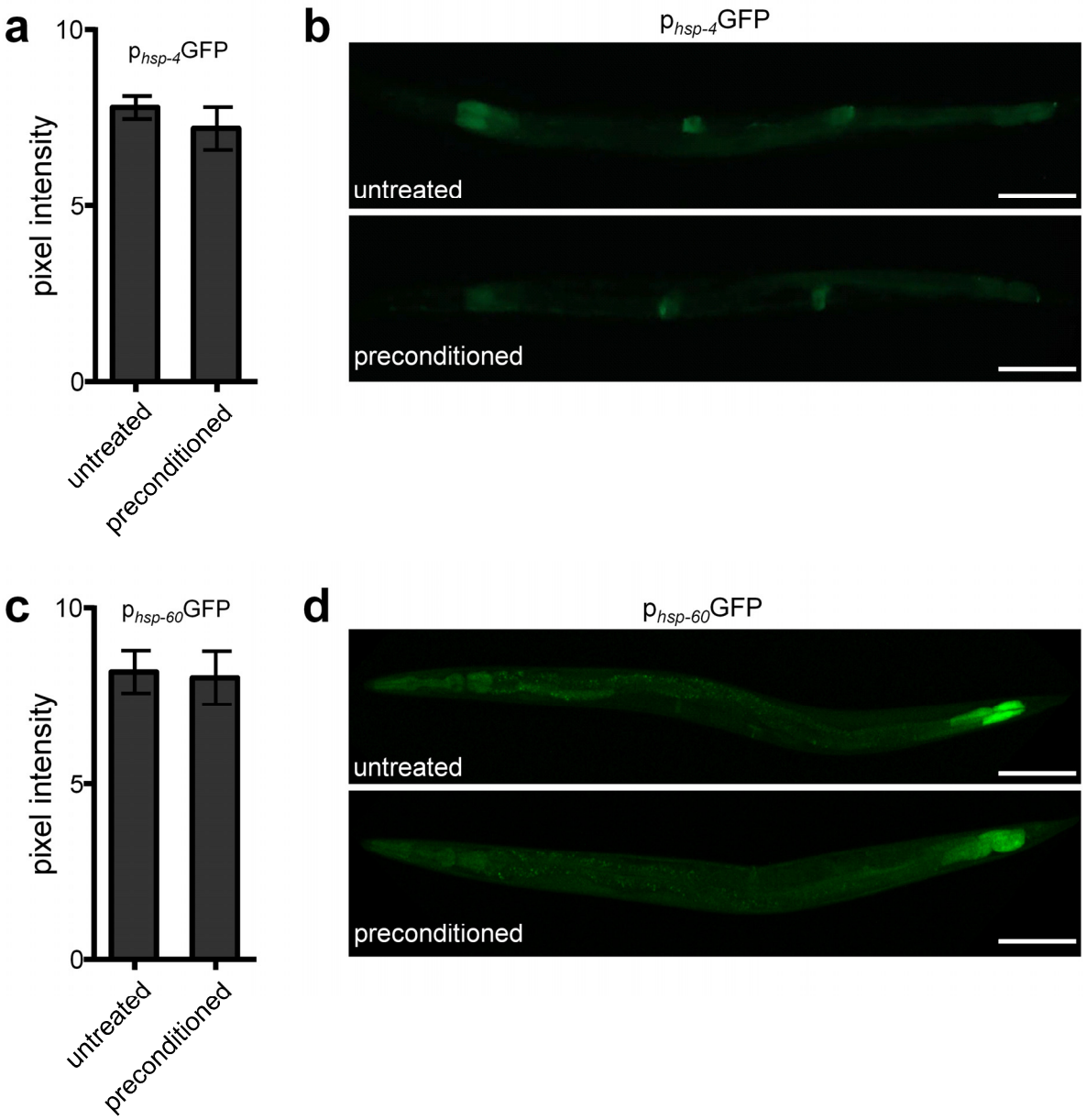

Figure S13 | Activation of the heat shock response pathway by incubation at 34°C for 30 min does not activate the ER or mitochondrial unfolded protein response (UPR). a, Fluorescence intensity of wild type animals expressing the p_{hsp-4}GFP transgene either without (untreated) or after heat preconditioning (*N*=50 animals per assay; *P*>0.05 for wt untreated vs. preconditioned; unpaired *t*-test). **b,** Confocal images of transgenic animals expressing the reporter p_{hsp-4}GFP under normal conditions (untreated, top panel) or after heat preconditioning (bottom panel). Bar denotes 100 μm. **c,** Fluorescence intensity of wild type animals expressing the p_{hsp-60}GFP transgene either without (untreated) or after heat preconditioning (*N*=50 animals per assay; *P*>0.05 for wt untreated vs. preconditioned; unpaired *t*-test). **d,** Confocal images of transgenic animals expressing the reporter p_{hsp-60}GFP under normal conditions (untreated, top panel) or after heat preconditioning (bottom panel). Bar denotes 100 μm. Error bars denote S.E.M. values.

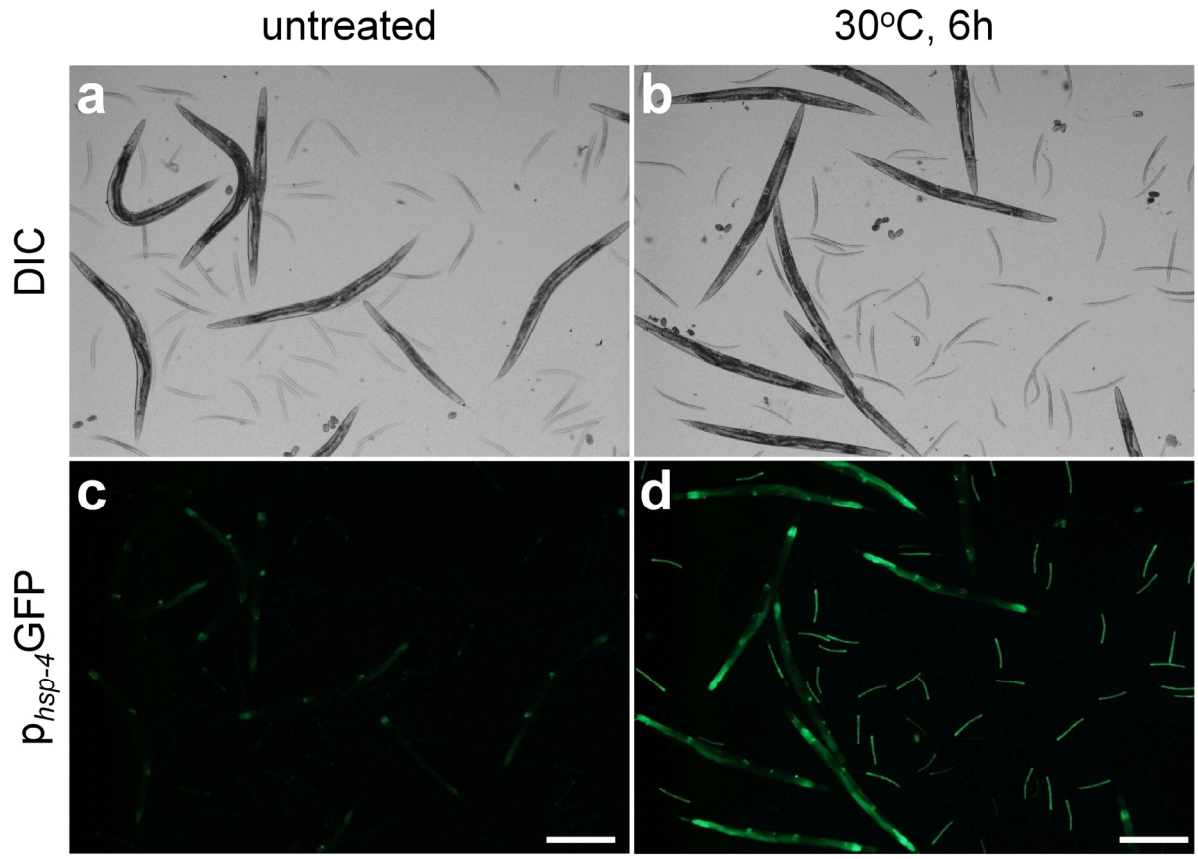

Figure S14 | Prolonged exposure to moderately elevated temperature activates distinct stress response pathways in addition to the heat shock response. DIC (**a, b**) and epifluorescence (**c, d**) images of transgenic animals expressing the UPR^{ER} reporter p_{hsp-4}GFP under normal conditions (untreated; a,c) and after incubation at 30°C for 6 h (b, d). Bar denotes 50 µm.

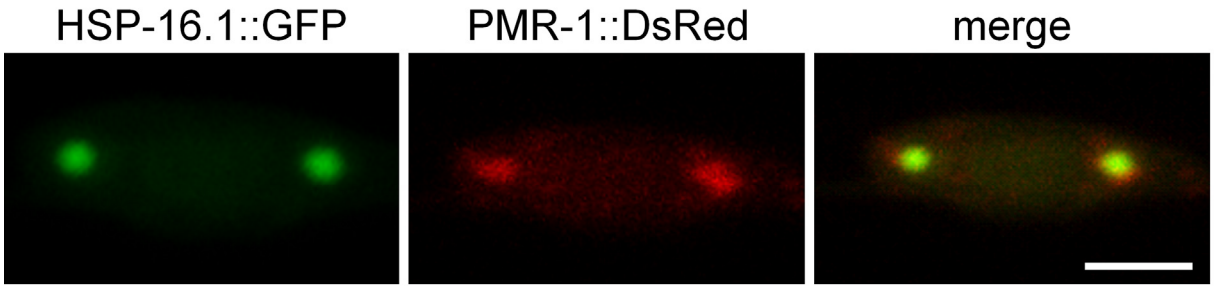

Figure S15 | HSP-16.1 colocalizes with PMR-1 in nematode neurons. Confocal images of *C. elegans* neurons expressing fluorescently tagged (GFP) HSP-16.1 along with fluorescently tagged (DsRed) PMR-1. Neuronal cell bodies are shown. Bar denotes 4 µm.

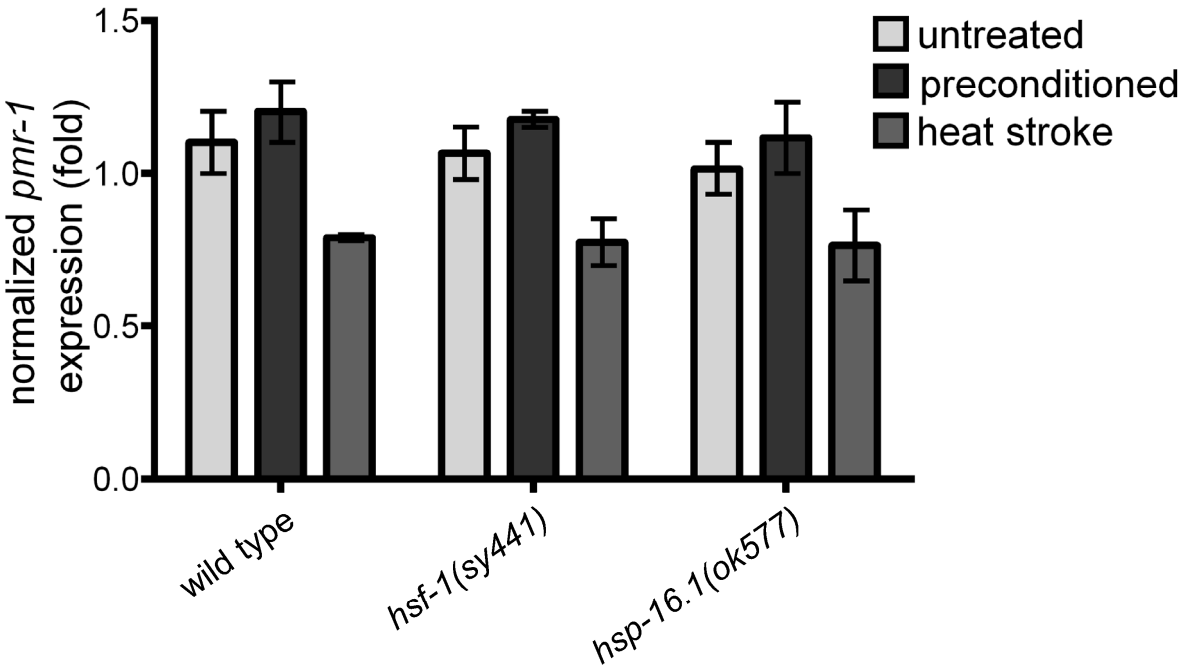

Figure S16 | *pmr-1* mRNA levels are not altered in mutants deficient for HSF-1 or HSP-16.1. Real time PCR analysis of *pmr-1* mRNA levels in wild type animals, *hsf-1(sy441)* mutants lacking HSF-1, and *hsp-16.1(ok577)* mutants lacking HSP-16.1, under normal conditions (untreated), after heat preconditioning, and after heat stroke (P>0.05 for wt preconditioned or heat stroked vs. *hsf-1(sy441)* or *hsp-16.1(ok577)* preconditioned or heat stroked; two-way ANOVA). Error bars denote S.E.M. values.

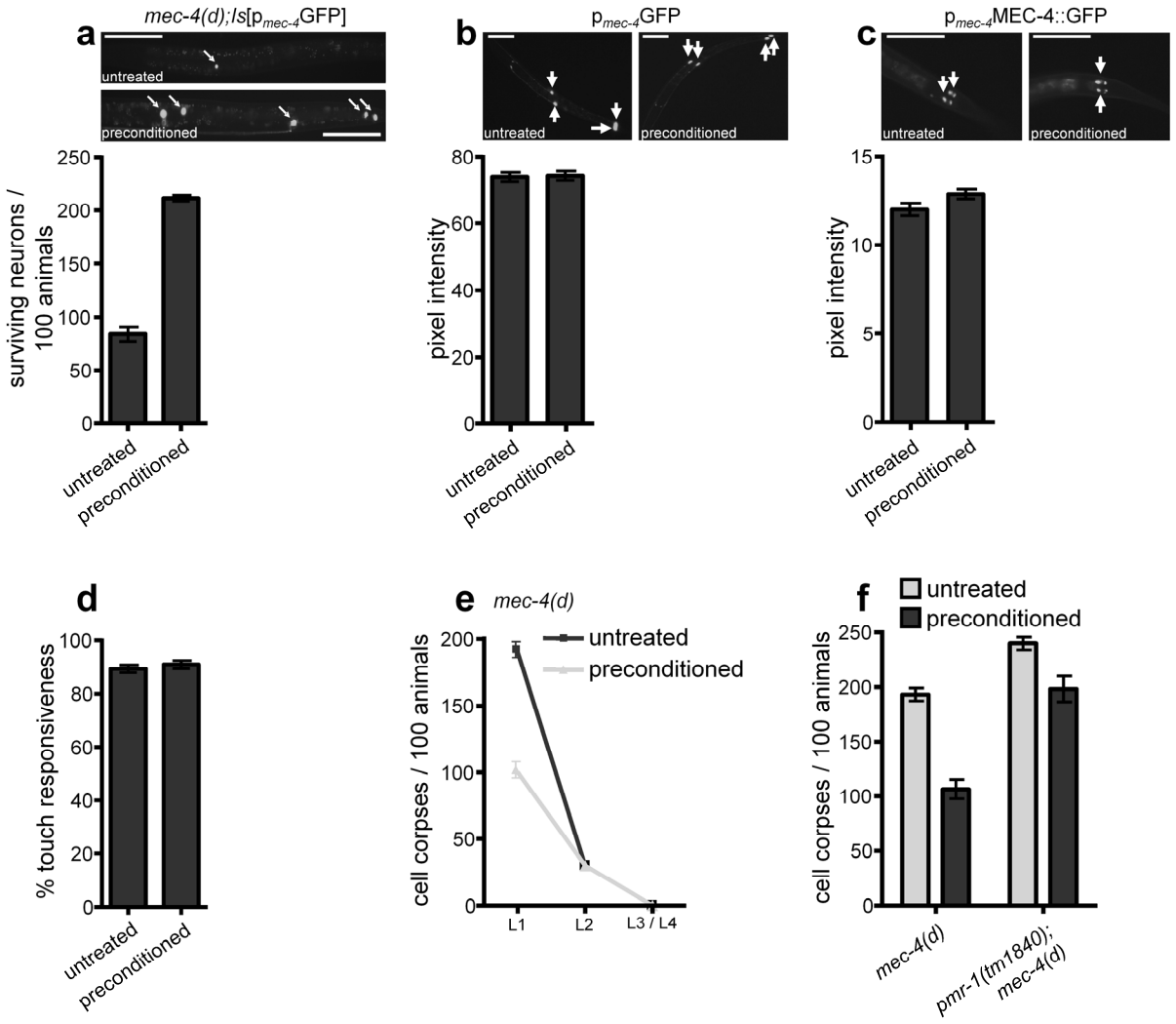

Figure S17 | Preconditioning does not interfere with the expression, stability or function of MEC-4. a, Survival of neurons during late developmental stages, per 100 animals carrying the neurotoxic *mec-4(d)* allele and expressing the p_{mec-4}GFP transgene either without (untreated) or after heat preconditioning (*N*=300 animals per assay; *P*<0.001 for *mec-4(d)*, untreated vs. preconditioned; unpaired *t*-test). Animals were preconditioned at the egg stage and subsequently grown at 26°C until the L4 stage of development. Fluorescent cells are either absent or barely visible in untreated *mec-4(d)* animals (top panel) whereas in preconditioned *mec-4(d)* animals, neurons escape necrotic cell death and survive until adulthood (bottom panel). Arrows point to touch receptor neurons. **b,** Fluorescence intensity of neurons of wild type animals expressing the p_{mec-4}GFP transgene either without (untreated) or after heat preconditioning (*N*=50 animals per assay; *P*>0.05 for wt untreated vs. preconditioned; unpaired *t*-test). Representative pictures of untreated (left panel) and preconditioned animals (right panel). Arrows point to touch receptor neurons. **c,** Fluorescence intensity of neurons of wild type animals expressing a translational fusion of *mec-4* to GFP

either without (untreated) or after preconditioning (*N*=50 animals per assay; *P*>0.05 for wt untreated vs. preconditioned; unpaired *t*-test). The membrane distribution of the MEC-4 channel is depicted in untreated (arrows, left panel) and preconditioned (arrows, right panel). Bars denote 20 μm. **d,** Responsiveness of wild type animals to five sequential gentle body touches at the head and tail region either without (untreated) or after heat preconditioning (*N*=250 animals per assay; *P*>0.05 for wt untreated vs. preconditioned; unpaired *t*-test). **e,** Time-course analysis of *mec-4(d)*-induced necrotic cell death without (untreated) or after heat preconditioning. The number of touch receptor neuron corpses, at the larval stages indicated, per 100 animals is graphed (*N*=300 animals per assay; *P*<0.001 for *mec-4(d)* untreated vs. preconditioned; unpaired *t*-test). **f,** Number of neuron corpses, at the L1 larval stage of development, per 100 *mec-4(d)* animals carrying a neurotoxic allele, and *pmr-1(tm1840);mec-4(d)* double mutants lacking PMR-1 hatched from untreated or preconditioned eggs (*N*=350; *P*<0.01 for *mec-4(d)* untreated vs. *pmr-1(tm1840);mec-4(d)* untreated; two-way ANOVA). Error bars denote S.E.M values.

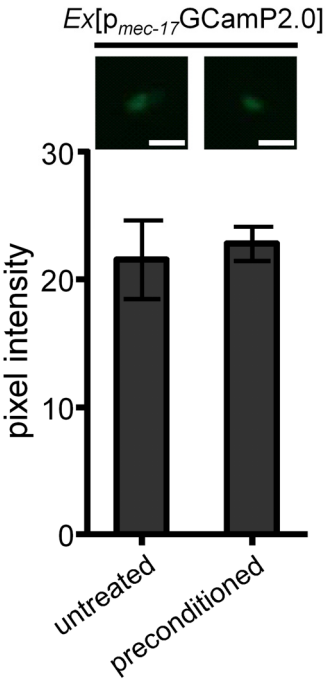

Figure S18 | Heat preconditioning does not perturb cytoplasmic Ca^{2+} levels. Ca^{2+} level-dependent fluorescence emission intensity from neurons expressing the Ca^{2+} reporter GCaMP2.0, in wild type animals, under normal conditions (untreated), and upon heat preconditioning (*N*=80 animals per assay; *P*>0.05 for untreated vs. preconditioned; unpaired *t*-test). Representative images of touch receptor neuron cell bodies are depicted above each condition. Images were acquired under the same exposure, using a 40x objective lens. Bar denotes 10 μm.

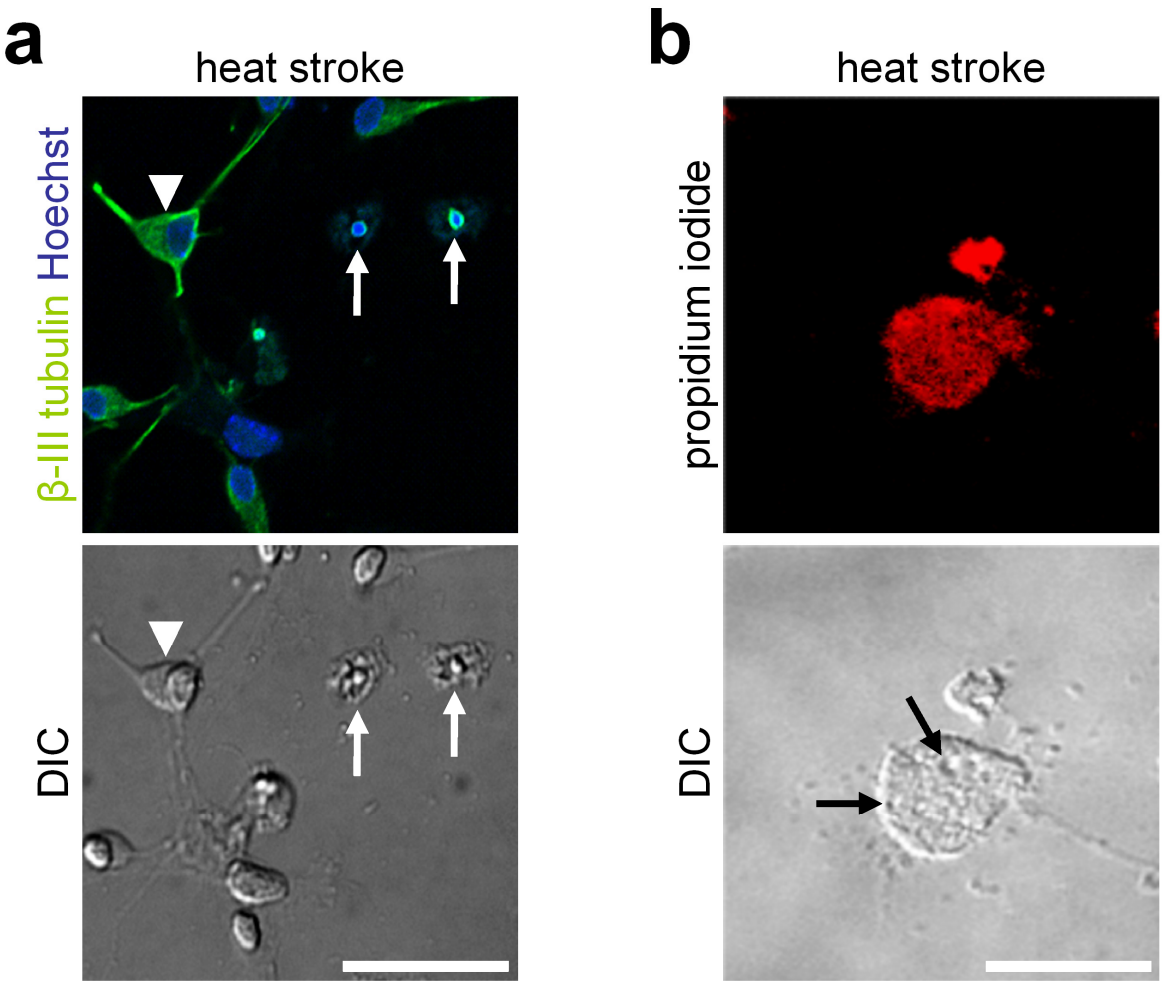

Figure S19 | Heat stroke induces necrotic cell death in ES cell-derived neurons. a, Fluorescence (top panel) and DIC (bottom panel) images of neurons undergoing heat stroke-induced degeneration. Neurons display swollen morphology and loss of integrity. Arrows denote neurons in advanced degeneration. Arrowhead denotes a neuron with preserved cell body, for comparison. Bar denotes 50 μm. **b,** Fluorescence (top panel) and DIC (bottom panel) image of a neuron stained with propidium iodide, after heat stroke. Note the necrotic, balloon-like morphology. Arrows indicate vacuoles. Bar denotes 20 μm.

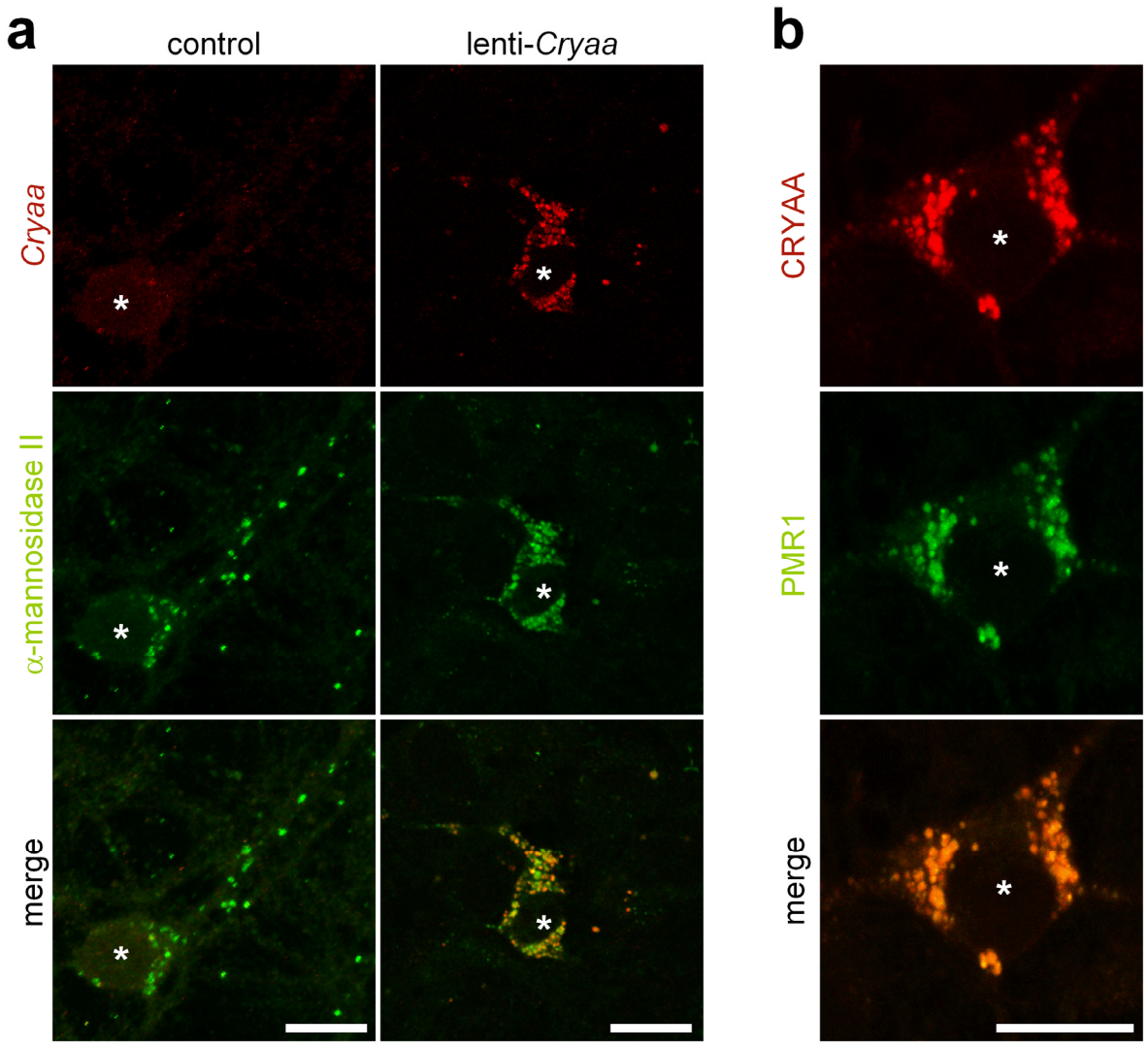

Figure S20 | Crystallin αA colocalizes with PMR1 in the Golgi of ES cell-derived neurons. a, Confocal images of ES cell-derived control and *Cryaa* overexpressing neurons immunostained for *Cryaa* and the Golgi marker α-mannosidase II. **b,** Confocal images of an ES cell-derived neuron, co-immunostained for CRYAA and PMR1. Asterisks denote the nucleus. Bars denote 20 μm.

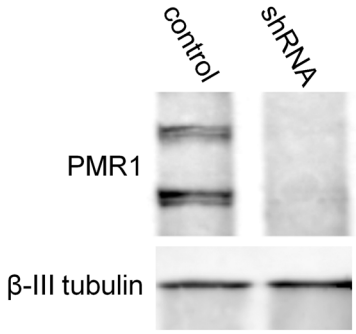

Figure S21 | RNAi-mediated downregulation of *Pmr1* in ES cell-derived neurons. Western blot analysis of PMR1 protein levels in control neurons and after *Pmr1* downregulation by shRNA. β-III tubulin was used as loading control.

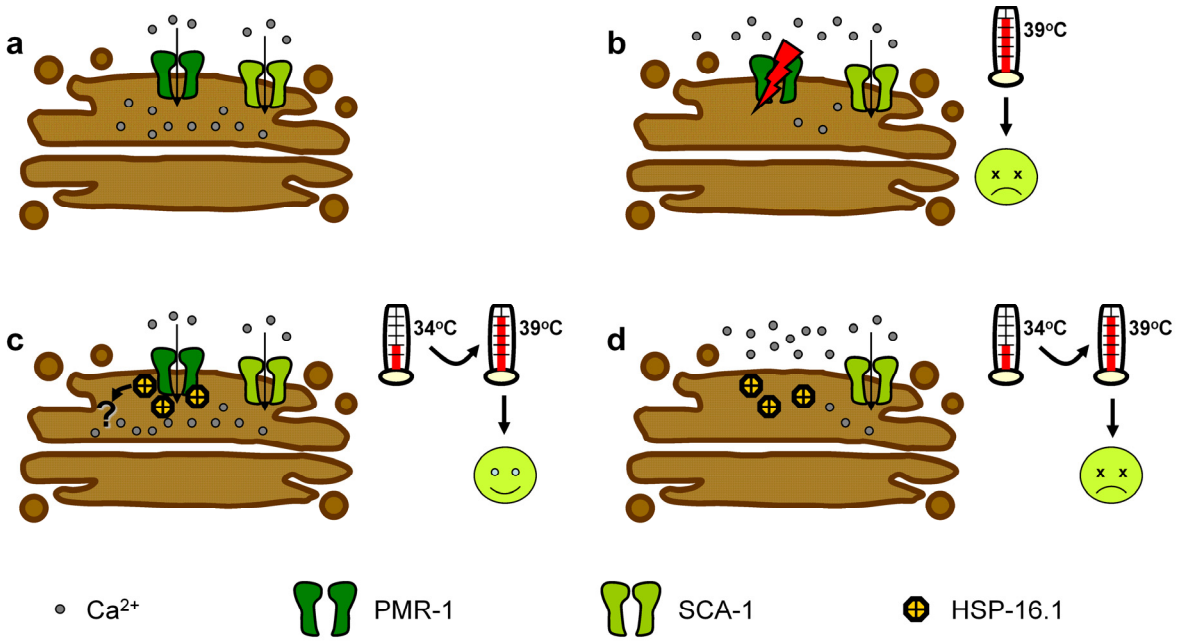

Figure S22 | Working model describing the protective mechanism of preconditioning against necrotic cell death triggered by heat stroke. The contribution of the medial Golgi (depicted as brown cisternae) to cytoplasmic Ca^{2+} homeostasis and consequently to cell survival is presented. **a,** Under normal conditions the Golgi P-type ATPase Ca^{2+}/Mn^{2+} pump PMR-1 (shown in dark green), synergizes with SCA-1 (shown in light green), and perhaps other unidentified Ca^{2+} pumps, to sequester Ca^{2+} (depicted as gray circles) inside Golgi and maintain cellular ionic balance. **b,** Exposure to extreme temperature (indicated by the thermometer pointing at 39°C), leads to increased cytoplasmic Ca^{2+} concentration, partly due to perturbation of the function of PMR-1 (indicated by red lightning), and consequently to cell death. Other intracellular Ca^{2+} stores might also contribute to the elevated Ca^{2+} concentration under stress conditions. Interestingly, PMR-1 depletion results in increased cytoplasmic Ca^{2+} concentration even under normal conditions (not shown). **c,** Preconditioning (indicated by the thermometer pointing at 34°C) induces the expression of *hsp-16.1* (indicated by the yellow polygon) which protects from uncontrolled cytoplasmic Ca^{2+} concentration increase after exposure to heat stroke conditions and eventually suppresses necrosis. This chaperone presumably restores the function of PMR-1 by preserving its proper conformation under stress conditions. HSP-16.1 might also have additional protective roles inside the Golgi (indicated by the question mark). **d,** In the absence of PMR-1, induced HSP-16.1 after preconditioning cannot confer its protective effect and heat stroke results in excess release of Ca^{2+} in the cytoplasm and cell death. Our results demonstrate that in addition to noxious heat, preconditioning exerts a protective effect against necrosis triggered by diverse insults, unrelated to thermal stress.